Spin-glass chain in a magnetic field : influence of the disorder distribution on ground state properties and low-energy excitations

Cécile Monthus and Thomas Garel

Service de Physique Théorique, Unité de recherche associée au CNRS,
DSM/CEA Saclay, 91191 Gif-sur-Yvette, France

For the spin-glass chain in an external field h, a non-zero weight at the origin of the bond distribution $\rho(J)$ is known to induce a non-analytical magnetization at zero temperature : for $\rho(J) \sim A|J|^{\mu-1}$ near $J \to 0$, the magnetization follows the Chen-Ma scaling $M \sim h^{\mu/(2+\mu)}$. In this paper, we numerically revisit this model to obtain detailed statistical information on the ground state configuration and on the low-energy two-level excitations that govern the low temperature properties. The ground state consists of long unfrustrated intervals separated by weak frustrated bonds: We accordingly compute the strength distribution of these frustrated bonds, as well as the length- and magnetization- distributions of the unfrustrated intervals. We find that the low-energy excitations are of two types (i) one frustrated bond of the ground state may have two positions that are nearly degenerate in energy (ii) two neighboring frustrated bonds of the ground state may be annihilated or created with nearly zero energy cost. For each excitation type, we compute its probability density as a function of its length. We moreover show that the contributions of these excitations to various observables (specific heat, Edwards-Anderson order parameter, susceptibility) are in full agreement with direct transfer matrix evaluations at low temperature. Finally, following the special bimodal case $\pm J$, where a Ma-Dasgupta RG procedure has been previously used to compute explicitly the above observables, we discuss the possibility of an extended RG procedure : we find that the ground state can be seen as the result of a hierarchical 'fragmentation' procedure that we describe.

I. INTRODUCTION

In this paper, we consider the one dimensional spin-glass chain in a small external field $h > 0$

$$H = -\sum_i J_i \sigma_i \sigma_{i+1} - h \sum_i \sigma_i \tag{1}$$

to obtain detailed results on the ground state and the low-energy excitations, as a function of the exponent $\mu > 0$ characterizing the weight of the coupling distribution for small couplings

$$\rho(J) \underset{J \to 0}{\simeq} A|J|^{\mu-1} \tag{2}$$

As is well-known, the previous model is equivalent to a random-bond and random-field ferromagnetic chain [4]

$$H = -\sum_i |J_i| S_i S_{i+1} - h \sum_i x_i S_i \tag{3}$$

where $x_i = \prod_{j=1}^i \text{sgn}(J_j)$.

A. Bimodal distribution $J_i = \pm J$: Imry-Ma argument and real-space RG

For the special case of the bimodal distribution $J_i = \pm J$ with probabilities $(1/2, 1/2)$, the model (3) corresponds to a pure Ising chain $|J_i| = J$ in a bimodal random field $h_i = h x_i = \pm h$. The Imry-Ma argument [1] for the random field Ising chain can be immediately translated for the spin-glass in external field, since the domain walls of the RFIM now becomes frustrated bonds for the spin-glass : the random magnetization m of an unfrustrated domain of length l is of order $m \sim \sqrt{l}$, i.e. it gives rise to an energy of order $2h\sqrt{l}$ in the external field h, whereas a pair of two frustrated bonds has for energy cost $4J$. As a consequence, the ground state is made of unfrustrated domains having the typical Imry-Ma length $L_{IM} \sim 4 J^2/h^2$. The real-space Ma-Dasgupta RG [2] allows to construct explicitly the positions of frustrated bonds and to compute various statistical properties, such as the distribution of the domain lengths. This approach moreover yields the statistics of low-energy two-level excitations [3]. A natural question is then : what are the corresponding results for a general distribution $\rho(J)$ that is not bimodal ? It turns out that a different behavior occurs if $\rho(J)$ has some weight at small couplings $J \sim 0$. This case, which includes the Gaussian distribution, completely changes the physics of the model, as we now discuss.

B. Distributions with small couplings $\rho(J) \simeq A|J|^{\mu-1}$: Chen-Ma argument

For distributions presenting some weight at small couplings (2) the above Imry-Ma argument for the bimodal case is replaced by the following Chen-Ma argument [4]. The essential idea is that frustrated bonds will be now located on weak bonds, in contrast with the bimodal case where the cost of a frustrated bond is the same everywhere. More precisely, the Chen-Ma (CM) argument is as follows : the bonds J_i weaker than some cut-off $|J_i| \leq J_{CM}$ are separated by a typical distance of order

$$l_{CM} \sim J_{CM}^{-\mu} \tag{4}$$

The magnetization of the unfrustrated domain between two such weak bonds is of order

$$m_{CM} \sim \sqrt{l_{CM}} \sim J_{CM}^{-\mu/2} \tag{5}$$

The flipping of such a domain thus involves a typical energy of order J_{CM} for the creation of two weak frustrated bonds, but allows to gain a magnetic energy of order $hm_{CM} \sim hJ_{CM}^{-\mu/2}$. The balance between the two terms yields an optimal cut-off of order [4]

$$J_{CM} \sim h^{2/(2+\mu)} \tag{6}$$

so that the magnetization per spin M_s presents the following non-analytical behavior

$$M_s \sim \frac{m_{CM}}{l_{CM}} \sim h^{\frac{\mu}{(2+\mu)}} \tag{7}$$

The zero-temperature susceptibility

$$\chi(T = 0) \sim \frac{M_s}{h} \sim h^{-2/(2+\mu)} \tag{8}$$

thus diverges at zero field $h \to 0$. For instance, the Gaussian distribution $\rho(J)$, which corresponds to the exponent $\mu = 1$, leads to the behavior $M_s \sim h^{1/3}$. The critical exponent $\frac{\mu}{(2+\mu)}$ for the magnetization in external field was found to be exact via transfer matrix calculations by Gardner and Derrida [5], where the prefactor was moreover computed. The presence of small couplings does induce interesting new properties for the ground state with respect to the bimodal case.

Chen and Ma have also analyzed the low temperature properties, in particular in the regime where the temperature T is much smaller than the typical energy J_{CM} of a domain. In this regime $T \ll J_{CM}$ (6), only a small fraction of two-level excitations will be excited : the density $\rho(E = 0)$ of excitations near zero energy can be estimated to scale as [4]

$$\rho(E = 0) \sim \frac{1}{l_{CM}} \times \frac{1}{J_{CM}} \sim J_{CM}^{\mu-1} \sim h^{2(\mu-1)/(2+\mu)} \tag{9}$$

where $1/l_{CM}$ represents the density of frustrated bonds in the ground state, and where $1/J_{CM}$ represents the fraction of these frustrated bonds that will be involved in excitations of vanishing energy $E \to 0$. This excitations density is then expected to govern the leading term of the specific heat at low temperature [6]

$$C \underset{T \to 0}{\simeq} T \frac{\pi^2}{6} \rho(E = 0) + O(T^2) \tag{10}$$

In this paper, our aim is to study in some details the statistical properties of the ground state configuration, and of the the low-energy excitations that govern the low-temperature properties.

II. STATISTICAL PROPERTIES OF THE GROUND STATE CONFIGURATION

In this section, we present the numerical results that we have obtained via the zero-temperature transfer-matrix formulation [5] from which one can obtain the ground state configuration $\{\sigma_i\}$ in each given sample $\{J_i\}$. In the whole paper, we have used the following distribution for the couplings

$$\rho(J) = \frac{\mu}{2}|J|^{\mu-1} \quad \text{for} \quad -1 \leq J \leq 1 \tag{11}$$

yielding $A = \frac{\mu}{2}$. The results given in this section have been obtained from averages over 10^5 independent chains containing $N \sim 10^6$ sites.
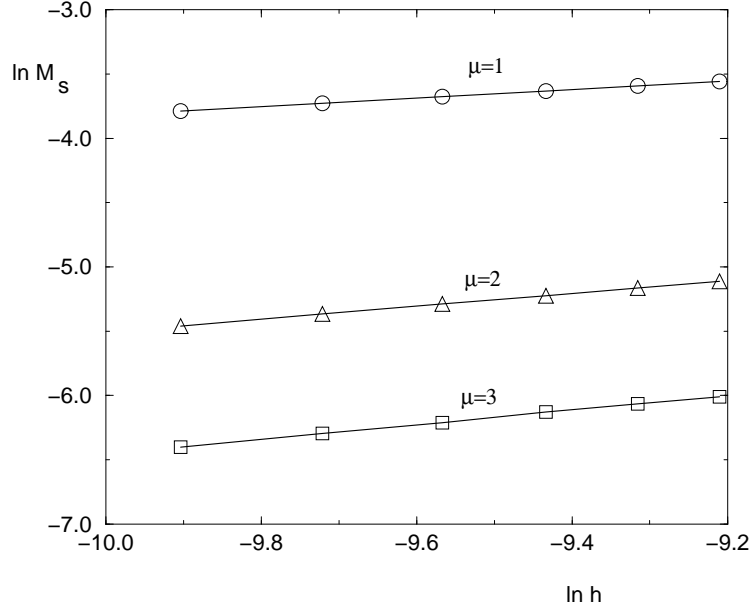
FIG. 1: Magnetization per spin in the ground state as a function of the external field varying between $h = 5.10^{-5}$ and $h = 1.10^{-4}$ in log-log plot, for disorder distributions (11) with exponents $\mu = 1, 2, 3$. The corresponding slopes are in full agreement with the exact exponents $1/3$, $1/2$, $3/5$ (Eq 12).

A.   Magnetization per spin

As a first observable, we have computed the magnetization per spin which corresponds to a thermodynamic quantity which is exactly known from a transfer matrix calculation done by Gardner and Derrida who have obtained [5]

$$M_s^{exact} \underset{h \to 0}{\simeq} (\mu + 1) \left(\frac{4A}{\mu(\mu + 2)^2} \right)^{\frac{1}{\mu+2}} \frac{\Gamma\left(\frac{\mu+1}{\mu+2}\right)}{\Gamma\left(\frac{1}{\mu+2}\right)} h^{\frac{\mu}{(2+\mu)}} \tag{12}$$

We have checked that both the scaling in h (see Figure 1) and the prefactor are in excellent agreement with the exact result (12).

Now that we have identified the regime in h where the scaling (7) is satisfied, we may turn to more refined statistical properties for which, to the best of our knowledge, no exact expression is available.

B.   Probability distribution of frustrated links

We have computed the normalized probability density of coupling $|J|$ among frustrated links

$$P^f(J) = \frac{N_f(J)}{\int dJ' N_f(J')} \tag{13}$$

where $N_f(J)$ represents the number of frustrated links of strength J.

According to the Chen-Ma argument, the frustrated links should have a typical strength of order $J_{CM} \sim h^{2/(2+\mu)}$. We have thus plotted on Figure 2 the probability distribution of frustrated links in terms the appropriate rescaled variable

$$K = \frac{|J|}{J_{CM}(h)} = \frac{|J|}{h^{2/(2+\mu)}} \tag{14}$$

for various h with the same initial distribution (11) corresponding to $\mu = 1$.

To compare the distributions of frustrated links corresponding to different disorder distributions $\rho(J)$ characterized by different exponents μ (11), it is more convenient to consider the reduced variable
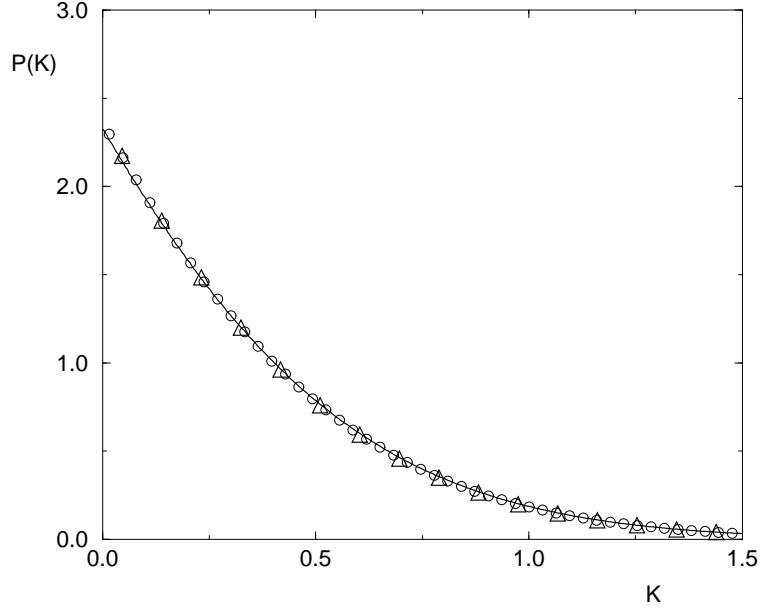
$$r = |J|^\mu \tag{15}$$

FIG. 2: Rescaled probability distributions $P_{\mu=1}(K = |J|/J_{CM}(h))$ of frustrated links in the ground state : the data for various fields, namely $h = 1.10^{-2}$ (line), $h = 5.10^{-4}$ (circles) and $h = 1.10^{-4}$ (triangles), follow the same master curve.
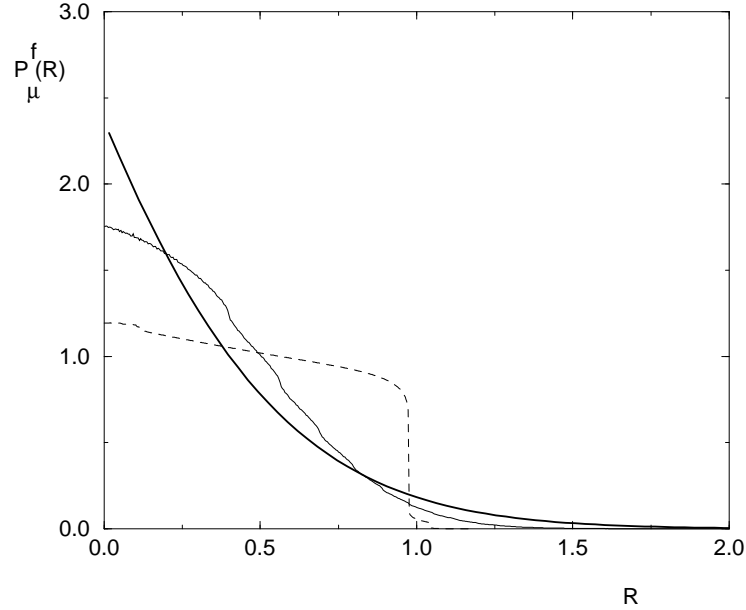

FIG. 3: Probability distributions $P_{\mu}^{f}(R \equiv r/r_{CM}(h) = (|J|/J_{CM}(h))^{\mu})$ of the frustrated links for various disorder distributions (11) corresponding to the exponents $\mu = 1$ (bold line), $\mu = 0.5$ (thin line) and $\mu = 0.1$ (dashed line).

which is distributed with the flat distribution

$$\pi^{apriori}(r) = \theta(0 \leq r \leq 1) \tag{16}$$

for any μ in (11). Taking into account the Chen-Ma scaling

$$r_{CM}(h) = J_{CM}^{\mu}(h) = h^{2\mu/(2+\mu)} \tag{17}$$

we have plotted on Figure 3 the probability distribution $P_{\mu}^{f}(R \equiv r/r_{CM}(h))$ of the frustrated links for various disorder distributions corresponding to the exponents $\mu = 1$, $\mu = 0.5$ and $\mu = 0.1$: for $\mu = 1$, this distribution is rather smooth, whereas it becomes steeper as μ decays. In particular, for $\mu = 0.1$, it becomes close to a simple theta function $\theta(R \leq 1)$.
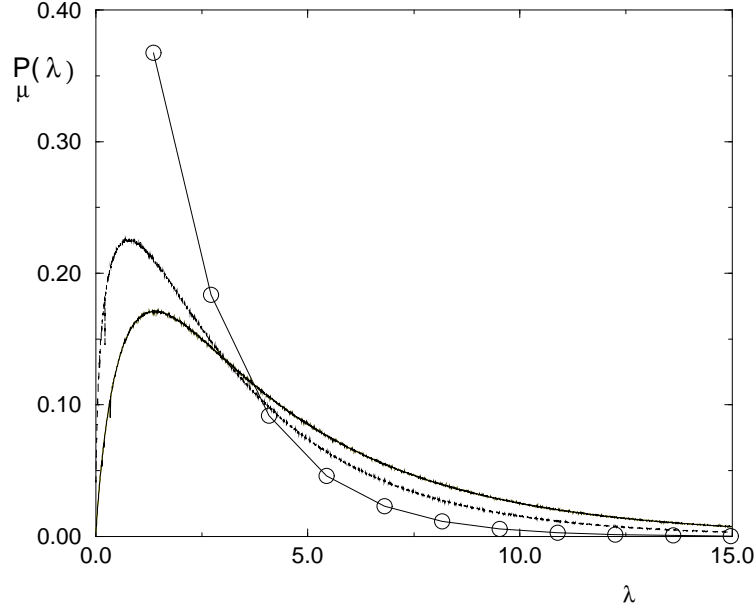
FIG. 4: Rescaled probability distributions $\mathcal{P}_\mu(\lambda = l/l_{CM(h)})$ of the length between two frustrated bonds of the ground state, for various initial disorder distribution characterized by the exponent $\mu = 1$ (full line) $\mu = 1/2$ (dashed line), $\mu = 1/4$ (circles)

This shows that in the limit $\mu \to 0$, the properties of the ground state become simpler, and we will discuss this point in more details in Appendix A.

C. Probability distribution of the lengths of unfrustrated intervals

According to the Chen-Ma argument, the length l between two frustrated links has for typical scale $l_{CM} \sim h^{-2\mu/(2+\mu)}$. Indeed, we obtain that the appropriate rescaled variable for the length of unfrustrated intervals is

$$\lambda = \frac{l}{l_{CM}(h)} = l h^{2\mu/(2+\mu)} \tag{18}$$

as h varies. The probability distribution $\mathcal{P}_\mu(\lambda)$ of the scaling variable λ is plotted on Figure 4 for various μ.

For $\lambda \to 0$, in contrast with the bimodal case where $\mathcal{P}(\lambda = l/l_{IM})$ presents an essential singularity [2], we obtain here power-law behavior near the origin

$$\mathcal{P}_\mu(\lambda) \underset{\lambda \to 0}{\propto} \lambda^{\alpha(\mu)} \tag{19}$$

with an exponent $\alpha(\mu)$ that grows with μ (see Figure 4). For instance for $\mu = 1$, the best fit yields the exponent $\alpha(\mu = 1) \simeq 0.8$. For large λ, the decay is exponential

$$\mathcal{P}_\mu(\lambda) \underset{\lambda \to \infty}{\propto} e^{-\gamma(\mu)\lambda} \tag{20}$$

For $\mu = 1$, the best fit yields $\gamma(\mu = 1) \simeq 0.25$.

D. Probability distribution of the magnetizations of unfrustrated intervals

Similarly, we find that, in agreement with the Chen-Ma argument, the appropriate rescaled variable for the magnetization of unfrustrated intervals is

$$\omega = \frac{m}{m_{CM}(h)} = m h^{\mu/(2+\mu)} \tag{21}$$

as h varies. The probability distribution $Q_\mu(\omega)$ of the scaling variable ω is plotted on Figure 5 for various μ.
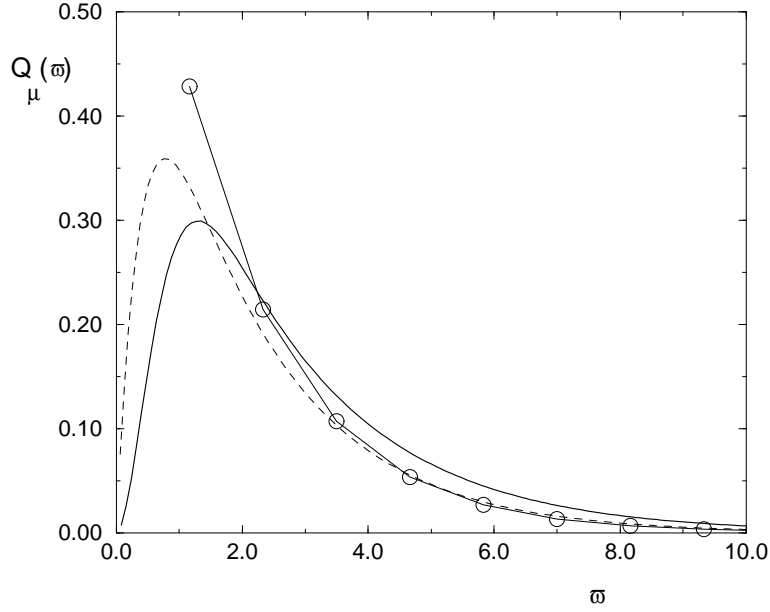
FIG. 5: Rescaled probability distributions $Q_\mu(\omega = m/m_{CM}(h))$ of the magnetization between two frustrated bonds of the ground state, for various initial disorder distribution characterized by the exponent $\mu = 1$ (full line) $\mu = 1/2$ (dashed line), $\mu = 1/4$ (circles).

Again, for $\omega \to 0$, we obtain power-law behaviors

$$Q_\mu(\omega) \underset{\omega \to 0}{\propto} \omega^{\beta(\mu)} \tag{22}$$

with for instance $\beta(\mu = 1) \sim 1.5$, whereas the decay for large ω is exponential

$$Q_\mu(\omega) \underset{\omega \to \infty}{\propto} e^{-\delta(\mu)\omega} \tag{23}$$

with $\delta(\mu = 1) \simeq 0.5$.

III. LOW-TEMPERATURE PROPERTIES

A. Low temperature transfer-matrix results for various observables

We have first computed via transfer matrix various observables in the low-temperature regime $T \ll J_{CM}(h)$ (6). For instance for $h = 0.02$ corresponding to $J_{CM}(h) = 0.07$, we have checked, for temperatures $T = 2.10^{-3}$, $T = 3.10^{-3}$, $T = 4.10^{-3}$, $T = 5.10^{-3}$, that the leading term of the specific heat is linear in T

$$C \equiv \frac{< E_N^2 > - < E_N >^2}{T^2 N} \underset{T \to 0}{\propto} T \tag{24}$$

and that the leading term of the susceptibility is a constant

$$\chi(T) \equiv \frac{< M_N^2 > - < M_N >^2}{T N} \underset{T \to 0}{\propto} cte \tag{25}$$

We have also found that the Edwards-Anderson order parameter deviates linearly in temperature from the zero-temperature value $q_{EA}(T = 0) = 1$

$$q_{EA} \equiv \overline{< \sigma_i >^2} \underset{T \to 0}{\simeq} 1 - T(cte') \tag{26}$$

We have then studied the dependence in the external field h at fixed temperature. For instance, for $T = 5.10^{-3}$, we have studied the dependence in $h = 10^{-2}$ to $h = 10^{-1}$ (see Figure 6). The results for the specific heat is in good
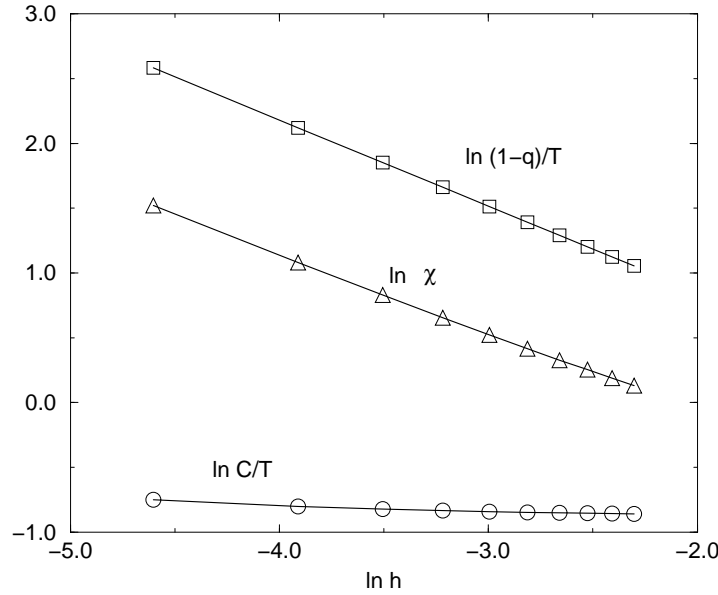
FIG. 6: Low temperature behaviors of the specific heat C, of the Edwards-Anderson order parameter q and of the susceptibility χ as a function of the external field in log-log plot for the special value $\mu = 1$: the exponents are respectively -0.04 for the specific heat, -0.66 for q and -0.6 for χ (see text for more details).

agreement with the Chen-Ma prediction (Eq 10 and 9)

$$\frac{C}{T} \underset{T \to 0}{\simeq} h^{2(\mu-1)/(2+\mu)} \tag{27}$$

as well as the susceptibility

$$\chi(T) \underset{T \to 0}{\simeq} h^{-2/(2+\mu)} \tag{28}$$

We have also computed the Edwards-Anderson order parameter, and found the same exponent as for the susceptibility (28)

$$\frac{1 - q_{EA}}{T} \underset{T \to 0}{\simeq} h^{-2/(2+\mu)} \tag{29}$$

which can be explained from the analysis in terms of the low-energy two-level excitations, as we now explain.

B. Interpretation in terms of low-energy two-level excitations

We have already given the expression (10) of the specific heat in terms of the density $\rho(E = 0)$ of excitations near zero energy. The similar expressions for the Edwards-Anderson order parameter and the susceptibility read [3]

$$\frac{1 - q_{EA}}{T} \underset{T \to 0}{\simeq} 2 \int_0^{+\infty} dl \; l\rho(E = 0, l) \tag{30}$$

$$\chi \underset{T \to 0}{\simeq} 2 \int_{-\infty}^{+\infty} dm \; m^2 \rho(E = 0, m) \tag{31}$$

where $\rho(E = 0, l)$ represents the density of excitations of length l, and where $\rho(E = 0, m)$ represents the density of excitations of magnetization m. Note that in the random field chain [3], the magnetization of a ferromagnetic domain is equal to its length, whereas here in the spin-glass chain, it is not the case, since the magnetization of an unfrustrated domain scales as $\sqrt{l}$. This is why the scaling in h are the same here for these two observables.
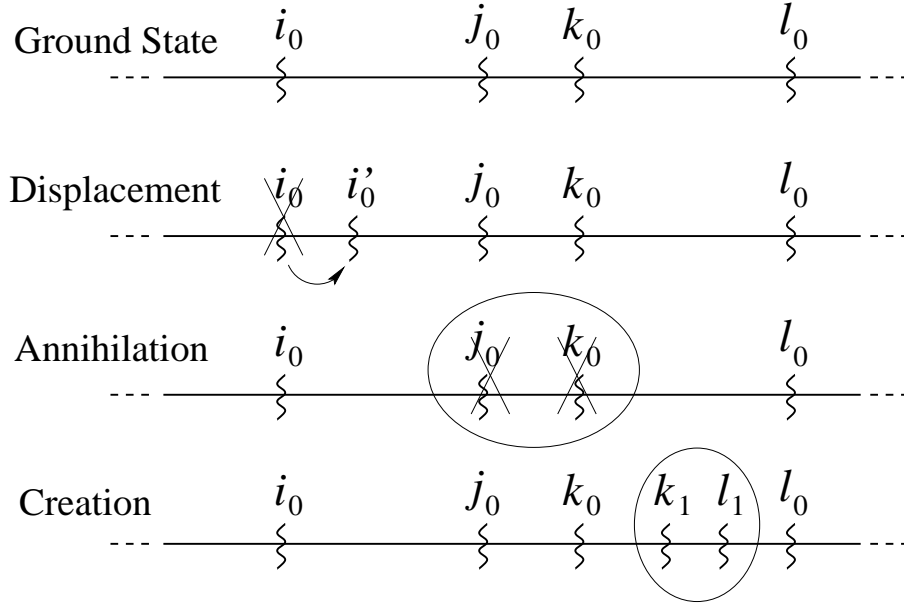
FIG. 7: Nature of the low-energy excitations. The ground state is made of long unfrustrated intervals separated by frustrated bonds called $..i_0, j_0, k_0, l_0....$ Low energy excitations may be of several types (displacement, annihilation or creation of frustrated bonds).

We have numerically computed the probability density of excitations, as a function of their size l and of their type. Indeed, we obtain by an exhaustive numerical enumeration that the total density of low-energy excitations is exactly the sum of three contributions

$$\rho_{tot}(E = 0, l) = \rho_{disp}^{(1)}(E = 0, l) + \rho_{anni}^{(2)}(E = 0, l) + \rho_{crea}^{(2)}(E = 0, l) \tag{32}$$

(1) The excitations of type 1, of density $\rho_{disp}^{(1)}(E = 0, l)$, involve a single frustrated link of the ground state, of coupling J_a, that can be displaced to another position of coupling J_b (inside the intervals defined by the two frustrated neighbors of J_a) with almost no energy cost. The energy difference

$$\Delta E^{(1)} = -2|J_a| + 2|J_b| + 2hm_{ab} \leq T \tag{33}$$

involves the defrustration of J_a, the frustration of J_b and the magnetization m_{ab} between these two links.

(2) The excitations of type 2 involves a pair of neighbor frustrated bonds that can be annihilated ($\rho_{anni}^{(2)}(E = 0, l)$) or that can be created ($\rho_{crea}^{(2)}(E = 0, l)$) with almost no energy cost

$$\Delta E_{anni}^{(2)} = -2|J_1| - 2|J_2| + 2hm_{12} \leq T \tag{34}$$

$$\Delta E_{crea}^{(2)} = 2|J_1| + 2|J_2| + 2hm_{12} \leq T \tag{35}$$

These two type of excitations are symmetric and are thus expected to correspond to the same distribution

$$\rho_{anni}^{(2)}(E = 0, l) = \rho_{crea}^{(2)}(E = 0, l) \tag{36}$$

which we have checked in our numerical results. The densities of these excitations in terms of their rescaled length $\lambda = l/l_{CM}(h)$ are given on Figure 8 for $\mu = 1$.

We have moreover checked the relations (10,30,31) between, on the one hand, the specific heat, the Edwards-Anderson order parameter, and the susceptibility obtained from low temperature transfer-matrix calculations, and on the other hand the total number of excitations, their averaged length, and their averaged square magnetization. The agreement shows that the excitations described above are the only ones that play a role in the low temperature behavior of these observables. The present analysis in terms of the statistics of low-energy excitations thus gives a microscopic interpretation of the low temperature equilibrium properties.
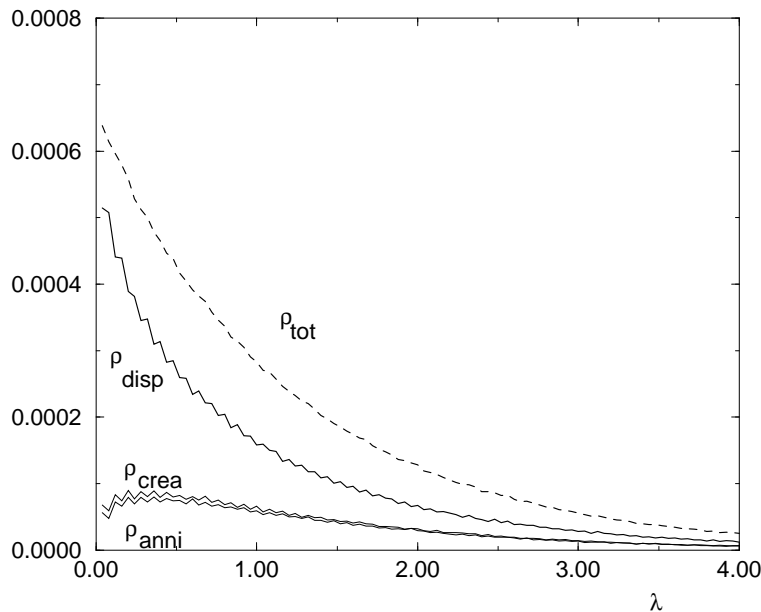
FIG. 8: Densities of the three types of low energy excitations present in equation (32), in terms of their rescaled length $\lambda = l/l_{CM}(h)$ in the case $\mu = 1$.

IV.   RENORMALIZATION PROCEDURES IN EACH SAMPLE

As already mentioned in the introduction, in the bimodal case $\pm J$, there exists a real-space RG procedure that allows to compute exactly the statistical properties of the ground state [2] (such as the domain length distribution) as well as the statistics of low-energy excitations [3]. A natural question is thus : is there a generalized RG procedure that would be valid for the spin-glass beyond the bimodal case $J_i = \pm J$? Before trying to answer this question for the $\rho(J) \sim A|J|^{\mu-1}$ case, let us first briefly recall the principle of the RG procedure for the bimodal case.

A.   Bimodal distribution

The RG procedure defined in ref [2] for the bimodal case, consists in an optimization from small scales towards large scales : one starts for instance from the completely magnetized state $\sigma_i = +1$, that contains many frustrated bonds, and one flips iteratively the unfrustrated domain presenting the smallest magnetization, as long as the energy is lowered, i. e. as long as the balance between the energy gained from the suppression of the two boundary frustrated bonds is bigger than the energy loss $(2hm)$ from the negative orientation with respect to the external field

$$\Delta E^{flip} = -4J + 2h|m| < 0 \tag{37}$$

So the RG procedure has to be stopped when all unfrustrated domains have magnetizations $m \geq 2J/h$: the state obtained then corresponds to the ground state. What makes the renormalization tractable in this case is that due to the constant cost $(2J)$ of any domain wall, the renormalization concerns a one-dimensional potential, namely the magnetization as a function of the running point.

B.   General distribution : hierarchical RG based on the energy

In this case, the problem cannot be reformulated as the renormalization of a one-dimensional potential, since in addition to the magnetization, one has to take into account that the couplings J_i vary along the chain. Moreover, we have seen with the Chen-Ma argument that the frustrated links are concentrated on small couplings.

As a first step, we can thus formulate the following renormalization that optimizes from the biggest scales towards smaller scales :

(i) one starts from the state with no frustrated links that presents a positive magnetization (of order $\sqrt{N}$ for a chain of size N) : it corresponds to one of the two mirror zero-field ground states.

(ii) at each step, we flip the interval $(\sigma_{i+1}, ...\sigma_j)$ that allows the maximal decrease of energy $E = \min\limits_{i<j} \Delta E(i,j) < 0$ where

$$\Delta E(i,j) = 2f(J_i)|J_i| + 2f(J_j)|J_j| + 2h \sum_{k=i+1}^{j} \sigma_k \tag{38}$$

where $f(J_i) = 1$ if J_i becomes frustrated during the flip, $f(J_i) = -1$ if J_i becomes unfrustrated during the flip. If we find no interval to flip, we have obtained the ground state, since by definition the ground state is stable upon the flip of any interval.

We have indeed checked that this procedure allows to obtain the exact ground state computed independently via the zero temperature transfer matrix. We have moreover obtained that actually, the links that become frustrated during the procedure never get 'unfrustrated' later in this procedure. And in fact the following hierarchical RG procedure, where at generation n, the chain is cut into a certain number of sub-chains, gives the exact ground state :

(i) same initial state as before

(ii) once the first interval (i_1, j_1) to be flipped is found, we can find the next intervals to be flipped independently within the three sub-chains $(1, i_1)$, (i_1, j_1) and (j_1, N). And we iterate until there is no interval to flip anymore.

The fact that the first links (i_1, j_1) that become frustrated indeed belongs to the final ground state, can be justified via a 'reductio ad absurdum' [7], and then it is valid for all stages of the procedure.

This hierarchical procedure thus defines an energy driven fragmentation process of the chain, whose statistical properties can be studied and compared to other fragmentation models [8]. In particular, we have studied the number n_{split} of splitting and the number n_{gene} of generations as a function of the size N of the chain, for $N = 500$ to $N = 8000$. For the disorder distribution (11) with $\mu = 1$ and external field $h = 0.02$, that corresponds to the length Chen-Ma scale $l_{CM}(h) \sim 13.5..$, we obtain, as expected, that the number of splittings grows linearly in N

$$\frac{n_{split}(N)}{N} \underset{N\to\infty}{\simeq} 8 \ 10^{-3} \tag{39}$$

and that the number of generations grows logarithmically in N

$$\frac{n_{gene}(N)}{\ln N} \underset{N\to\infty}{\simeq} 2.1 \tag{40}$$

This RG analysis reveals a hierarchical structure among the frustrated links of the ground state. This hierarchy has both a spatial meaning, but also an energy meaning. Indeed, since an interval created inside another interval has, by definition of the RG procedure, a smaller energy, it is clear that the low-energy excitations of the type 'annihilation' introduced in (32) can only concern a pair of frustrated bonds that have been created together and that have no descendent in the hierarchy. Similarly, the low-energy excitations of the type 'creation' introduced in (32) correspond to a pair of frustrated bonds that would have been created next if the procedure had been applied a bit beyond $\Delta E \leq 0$. Finally, the only remaining excitations are the 'displacements' (32), that actually also preserve the hierarchical structure, since a link can move only between its two frustrated neighbors.

C. RG based on the weakest link at each step

Since the frustrated links concentrate on the links that are weak, i.e. of order $J_{CM}(h)$, it is tempting to try to define a RG procedure based on the weakest link at each step. In Appendix A, we show that a simple RG procedure based on this idea becomes exact in the limit $\mu \to 0$, that corresponds to an infinitely broad distribution (11) near $J \to 0$.

V. CONCLUSION

For the spin-glass chain in an external field h, we have first studied via zero-temperature transfer-matrix calculations the statistical properties of the ground state configuration. We have then studied the nature and the statistics of the low-energy two-level excitations, via a direct enumeration, and we have analyzed their contribution to the specific heat, the Edwards-Anderson order parameter and the susceptibility in the low-temperature regime. Finally, we have shown that an extended RG procedure, based on the iterative flipping of the best energetic interval, could be used to obtain the exact ground state in external field. This RG procedure reveals a hierarchical structure among the frustrated links present in the ground state.

The possible relation of this hierarchical picture with higher dimensional disordered models is clearly of interest. In the 2d random field Ising model, a spatial hierarchical picture has been identified long ago [9], based on the existence of the Imry-Ma domain length scale. We tend to think that this hierarchy is energetic in nature. More precisely, we believe that a RG procedure that would start from the ferromagnetic pure state, and flip iteratively, at each step, the most advantageous domain- regardless of its size- will ultimately converge towards the ground state. After the initial flipping of the most advantageous domain (which, through the Imry-Ma argument, is also the largest), one has to search separately for the next advantageous domains inside and outside the initial one. These flipped domains will then display a disjoint or hierarchically nested structure. Another related problem, where an iterative optimization procedure starts from the largest scale and hierarchically proceeds towards smaller scales, has been studied by Binder [10] for interfaces.

For the 2d or 3d spin glass case at zero magnetic field, there is no equivalent of the Imry-Ma or Chen-Ma length scale. The existence of a hierarchical organization in ground state or low temperature properties has nevertheless been found along various lines: rigidity properties [11], distance between spin configurations subject to the same thermal noise [12, 13], calculations on small systems [14], extensive data clustering analysis [15]. This hierarchical organization pertains to spin clusters, and is not a priori linked to a hierarchy in their flipping energies [16].

VI. ACKNOWLEDGMENTS

APPENDIX A: SIMPLE SOLUBLE RG PROCEDURE IN THE LIMIT $\mu \to 0$

In the limit $\mu \to 0$, the disorder distribution $\rho(J)$ (11) becomes infinitely broad distribution near $J \to 0$. It is thus tempting to define a RG procedure based on the weakest link at each step. In the following, we consider the simplified RG procedure :

(i) same initial state as before : one starts from the state with no frustrated links that presents a positive magnetization

(ii) First iteration : we choose the smallest coupling in absolute value $\Gamma = |J_{min}|$. The chain is thus decomposed into two sub-chains. We consider the magnetizations of the two sub-chains $m_1 + m_2 = M > 0$: if one of the two magnetizations (m_1, m_2) is negative, for instance, $m_1 < 0$, we will flip the sub-chain 1 if it lowers the energy, i.e. if the balance between the cost 2Γ of introducing a frustrated bond between the two sub-chains is less than the energy gained by the orientation of the sub-chain 1 along the external field

$$\Delta E^{flip} = -2h|m_1| + 2\Gamma < 0 \tag{A1}$$

otherwise, if $\Delta E^{flip} > 0$, we do not flip the sub-chain 1. After this, the two sub-chains will evolve as two independent sub-chains with free boundary conditions, so we iterate the procedure.

This very simple RG procedure is of course not exact, since at each step, we neglect the weak bond at the other boundary of the interval that has been previously decimated $|J| < \Gamma$. Indeed, at each step, we consider that the cost of the flipping of an interval is exactly 2Γ, whereas it should be $2(\Gamma \pm \epsilon)$, where $\epsilon < \Gamma$ is the absolute value of the coupling at the other boundary, that has been previously decimated, and where the sign $(\pm)$ depends on the state of this coupling ϵ, frustrated or not, in the renormalized chain at the RG scale Γ. However, we will show below that it becomes exact in the limit $\mu \to 0$, where the distribution becomes infinitely broad distribution near $J \to 0$.

1. Statistical properties of the intervals between weak bonds at RG scale Γ

In this section, we study the RG procedure defined above in the thermodynamic limit of an infinite chain. At the renormalization scale Γ, the chain is split into independent unfrustrated intervals, separated by weak bonds that can be either frustrated or not. We now derive some statistical properties of these intervals between weak bonds.

The distribution $P_\Gamma(l)$ of the length $(j - i)$ between two weak bonds $J_{i,j} < \Gamma$ is simply exponential, since it corresponds to the probability that l independent couplings have $|J_k| \geq \Gamma$,

$$P_\Gamma(l) \simeq \frac{1}{l_\Gamma} e^{-\frac{l}{l_\Gamma}} \tag{A2}$$

with the characteristic length

$$l_\Gamma = \frac{1}{-\ln\left[1 - \int_{|J| \le \Gamma} dJ \rho(J)\right]} \underset{\Gamma \to 0}{\simeq} \frac{\mu}{2A\Gamma^\mu} \tag{A3}$$

The magnetization of an unfrustrated interval of length l is simply the sum $m = \pm \sum_{i=1}^l sgn(J_i)$. Since l is large, the distribution of m given l is a Gaussian in the ground state at $h = 0$, and thus we obtain after averaging with respect to the length l with (A2) the following a priori distribution

$$P_\Gamma^{apriori}(m) \simeq \int_0^{+\infty} dl \frac{1}{l_\Gamma} e^{-\frac{l}{l_\Gamma}} \frac{e^{-\frac{m^2}{2l}}}{\sqrt{2\pi l}} = \frac{1}{2m_\Gamma} e^{-\frac{|m|}{m_\Gamma}} \tag{A4}$$

with the characteristic magnetization

$$m_\Gamma = \sqrt{\frac{l_\Gamma}{2}} \underset{\Gamma \to 0}{\simeq} \frac{1}{2\Gamma^{\frac{\mu}{2}}} \left(\frac{\mu}{A}\right)^{\frac{1}{2}} \tag{A5}$$

Now from this a priori distribution that describes the magnetizations of these domains in the $h = 0$ ground state, we wish to compute the distribution of domain magnetizations obtained via the renormalization procedure, where we have tried to flip intervals in a iterative way.

A domain existing at scale Γ was created at some previous scale Γ' representing the biggest of the couplings at the two boundaries. Since the distribution of the already decimated coupling reads

$$\rho_\Gamma^{small}(|J|) = \frac{\theta(|J| < \Gamma)\rho(|J|)}{\int dJ \theta(|J| < \Gamma)\rho(|J|)} = \theta(|J| < \Gamma)\frac{\mu|J|^{\mu-1}}{\Gamma^\mu} \tag{A6}$$

the distribution of the creation scale Γ' is simply

$$\rho_\Gamma^{creation}(\Gamma') = 2\rho_\Gamma^{small}(\Gamma') \int_{|J'| < \Gamma'} d|J'|\rho_\Gamma^{small}(|J'|) = \theta(\Gamma' < \Gamma)\frac{2\mu(\Gamma')^{2\mu-1}}{\Gamma^{2\mu}} \tag{A7}$$

The stability condition $m > -\frac{\Gamma'}{h}$ at the scale Γ' of its creation immediately yields the simple properties for the probability distribution $P_\Gamma(m)$ of the domain magnetization at scale Γ

$$\theta\left(m > \frac{\Gamma}{h}\right) P_\Gamma(m) = 2P_\Gamma^{apriori}(m) \tag{A8}$$

$$\theta\left(-\frac{\Gamma}{h} > m\right) P_\Gamma(m) = 0 \tag{A9}$$

For the values $|m| < \Gamma/h$, the probability distribution $[P_\Gamma(m)]^{stable}$ induced by the only condition to have been stable at the creation scale Γ' reads

$$\theta\left(\frac{\Gamma}{h} > m > 0\right)[P_\Gamma(m)]^{stable} = P_\Gamma^{apriori}(m) \int_0^\Gamma d\Gamma' \frac{2\mu(\Gamma')^{2\mu-1}}{\Gamma^{2\mu}} \left[1 + \theta\left(m > \frac{\Gamma'}{h}\right)\right] \tag{A10}$$

$$= P_\Gamma^{apriori}(m)\left[1 + \left(\frac{mh}{\Gamma}\right)^{2\mu}\right] \tag{A11}$$

$$\theta\left(0 > m > -\frac{\Gamma}{h}\right)[P_\Gamma(m)]^{stable} = P_\Gamma^{apriori}(m) \int_0^\Gamma d\Gamma' \frac{2\mu(\Gamma')^{2\mu-1}}{\Gamma^{2\mu}} \left[\theta\left(0 > m > -\frac{\Gamma'}{h}\right)\right] \tag{A12}$$

$$= P_\Gamma^{apriori}(m)\left[1 - \left(\frac{|m|h}{\Gamma}\right)^{2\mu}\right] \tag{A13}$$

In the limit $\mu \to 0$, we have thus the simplification that negative m become negligible, because two bonds weaker than Γ are typically much weaker than Γ, as a consequence of the broadness of distribution. So at leading order in μ, we have the simple property

$$[P_\Gamma(m)]^{stable} \underset{\mu \to 0}{\simeq} = \theta(m \ge 0)2P_\Gamma^{apriori}(m) \tag{A14}$$

$$= \theta(m \ge 0)\frac{1}{m_\Gamma} e^{-\frac{|m|}{m_\Gamma}} \tag{A15}$$

2. Probability measure for the fragmentation process at scale Γ

The probability measure to find a bond of strength Γ inside an interval (L, M) existing at scale Γ^- that becomes fragmented into two sub-intervals (l_1, m_1) and (l_2, m_2) reads

$$\mathcal{N}_\Gamma(L, M; l_1, m_1; l_2, m_2) d\Gamma dL dl_1 dl_2 dm_1 dm_2 \tag{A16}$$

$$= d\Gamma \rho_\Gamma(\Gamma) \frac{dL}{l_\Gamma} e^{-\frac{L}{l_\Gamma}} dl_1 dl_2 \delta(L - (l_1 + l_2)) dM 2\theta(M \geq 0) dm_1 \frac{e^{-\frac{m_1^2}{2l_1}}}{\sqrt{2\pi l_1}} dm_2 \frac{e^{-\frac{m_2^2}{2l_2}}}{\sqrt{2\pi l_2}} \delta(M - (m_1 + m_2)) \tag{A17}$$

Indeed, we have the following properties, for the integration over some variables. After the integration over (m_1, m_2), the distribution of M is a Gaussian as it should

$$\int dm_1 \int dm_2 \mathcal{N}_\Gamma(L, M; l_1, m_1; l_2, m_2) = \tag{A18}$$

$$\rho_\Gamma(\Gamma) \frac{1}{l_\Gamma} e^{-\frac{L}{l_\Gamma}} \delta(L - (l_1 + l_2)) 2\theta(M \geq 0) \frac{e^{-\frac{M^2}{2L}}}{\sqrt{2\pi L}} \tag{A19}$$

After the integration over all magnetizations $(m_1, m_2.M)$, the distribution for (l_1, l_2) is uniform except for the constraint $l_1 + l_2 = L$

$$\int dM \int dm_1 \int dm_2 \mathcal{N}_\Gamma(L, M; l_1, m_1; l_2, m_2) = \tag{A20}$$

$$\rho_\Gamma(\Gamma) \frac{1}{l_\Gamma} e^{-\frac{L}{l_\Gamma}} \delta(L - (l_1 + l_2)) \tag{A21}$$

After the integration over (l_1, l_2), the probability to find a bond Γ in an interval of length L

$$\int dl_1 \int dl_2 \int dM \int dm_1 \int dm_2 \mathcal{N}_\Gamma(L, M; l_1, m_1; l_2, m_2) = \rho_\Gamma(\Gamma) \frac{1}{l_\Gamma} e^{-\frac{L}{l_\Gamma}} L \tag{A22}$$

is proportional to $L P_\Gamma(L)$ since they are L possible positions.

In the following, when computing observables concerning the flips at scale Γ, it will be more convenient to integrate first over the lengths that play no direct role in the flip condition, to keep the magnetizations that enters the flip condition

$$\mathcal{N}_\Gamma(M; m_1, m_2) \equiv \int dL \int dl_1 \int dl_2 \mathcal{N}_\Gamma(L, M; l_1, m_1; l_2, m_2) \tag{A23}$$

$$= \rho_\Gamma(\Gamma) \frac{1}{l_\Gamma} 2\theta(M \geq 0) \delta(M - (m_1 + m_2)) \int_0^{+\infty} dl_1 e^{-\frac{l_1}{l_\Gamma}} \frac{e^{-\frac{m_1^2}{2l_1}}}{\sqrt{2\pi l_1}} \int_0^{+\infty} dl_2 e^{-\frac{l_2}{l_\Gamma}} \frac{e^{-\frac{m_2^2}{2l_2}}}{\sqrt{2\pi l_2}} \tag{A24}$$

$$= \rho_\Gamma(\Gamma) \theta(M \geq 0) \delta(M - (m_1 + m_2)) e^{-\frac{|m_1|}{m_\Gamma}} e^{-\frac{|m_2|}{m_\Gamma}} \tag{A25}$$

3. Flipping probability at scale Γ

The number of bonds of strength Γ that becomes frustrated at scale Γ is proportional to

$$N_\Gamma^{frus}(\Gamma) = \int dM \int dm_1 \int dm_2 \mathcal{N}_\Gamma(M; m_1, m_2) \left[\theta\left(m_1 < -\frac{\Gamma}{h}\right) + \theta\left(m_2 < -\frac{\Gamma}{h}\right) \right] \tag{A26}$$

$$= \rho_\Gamma(\Gamma) \int dM \theta(M \geq 0) \int dm_1 e^{-\frac{|m_1|}{m_\Gamma}} e^{-\frac{|M - m_1|}{m_\Gamma}} 2\theta\left(m_1 < -\frac{\Gamma}{h}\right) \tag{A27}$$

$$= 2\rho_\Gamma(\Gamma) \int_0^{+\infty} dM e^{-\frac{M}{m_\Gamma}} \int_{\frac{\Gamma}{h}}^{+\infty} dm_1' e^{-2\frac{m_1'}{m_\Gamma}} \tag{A28}$$

$$= \rho_\Gamma(\Gamma) m_\Gamma^2 e^{-\frac{\Gamma}{h m_\Gamma}} \tag{A29}$$

that should be compared with the total number of bonds of strength Γ proportional to the normalization

$$
\begin{aligned}
N_\Gamma^{tot}(\Gamma) \quad &= \int dM \int dm_1 \int dm_2 \mathcal{N}_\Gamma(M; m_1, m_2) \tag{A30}\\
&= \rho_\Gamma(\Gamma) \int_0^{+\infty} dM \left[\int_{-\infty}^0 dm_1 e^{\frac{m_1}{m_\Gamma}} e^{-\frac{M-m_1}{m_\Gamma}} + \int_0^M dm_1 e^{-\frac{m_1}{m_\Gamma}} e^{-\frac{M-m_1}{m_\Gamma}} + \int_M^{+\infty} dm_1 e^{-\frac{m_1}{m_\Gamma}} e^{-\frac{m_1-M}{m_\Gamma}} \right] \tag{A31}\\
&= 2\rho_\Gamma(\Gamma) m_\Gamma^2 \tag{A32}
\end{aligned}
$$

The flipping probability $F_\Gamma(\Gamma)$ of a bond Γ at scale Γ is given by the ratio of the two

$$
F_\Gamma(\Gamma) = \frac{N_\Gamma^{frus}(\Gamma)}{N_\Gamma^{tot}(\Gamma)} = \frac{1}{2} e^{-\frac{\Gamma}{h m_\Gamma}} = \frac{1}{2} e^{-x} \tag{A33}
$$

where the rescaled variable

$$
x = \frac{\Gamma}{h m_\Gamma} = \frac{2}{h} \left(\frac{A}{\mu} \right)^{1/2} \Gamma^{1+\frac{\mu}{2}} \tag{A34}
$$

represents the ratio between the quantity Γ/h appearing in the flip condition and the typical scale m_Γ of the magnetization of a domain existing at scale Γ. At the beginning of the procedure $x \ll 1$, there is a finite probability of flip, of order $1/2$, whereas for $x \gg 1$, the probability of flip becomes exponentially small.

4. Magnetization per spin at the end of the procedure

To compute the magnetization per spin $m_{spin}(h)$, we have to integrate over all the flips done at various scales, and to keep track of the associated magnetization gain

$$
m_{spin}(h) \quad = \sum_\Gamma \frac{\sum_i \Delta m_i}{\sum_i l_i} = \int_0^{+\infty} \frac{(\Delta m)_{\Gamma, \Gamma + d\Gamma}}{l_\Gamma} \tag{A35}
$$

where $(\Delta m)_{\Gamma, \Gamma + d\Gamma}$ is the mean magnetization gain associated to a domain flip at scale Γ, which can be expressed in terms of the measure (A25)

$$
\begin{aligned}
(\Delta m)_{\Gamma, \Gamma + d\Gamma} &= \int dM \int dm_1 \int dm_2 \mathcal{N}_\Gamma(M; m_1, m_2) \left[\theta \left(m_1 < -\frac{\Gamma}{h} \right) 2|m_1| + \theta \left(m_2 < -\frac{\Gamma}{h} \right) 2|m_2| \right] \tag{A36}\\
&= \rho_\Gamma(\Gamma) \int dM \theta(M \geq 0) \int dm_1 e^{-\frac{|m_1|}{m_\Gamma}} e^{-\frac{|M-m_1|}{m_\Gamma}} \theta \left(m_1 < -\frac{\Gamma}{h} \right) 4|m_1| \tag{A37}\\
&= 4\rho_\Gamma(\Gamma) \int_0^{+\infty} dM e^{-\frac{M}{m_\Gamma}} \int_{\frac{\Gamma}{h}}^{+\infty} dm_1' \, m_1' e^{-2\frac{m_1'}{m_\Gamma}} \tag{A38}\\
&= \rho_\Gamma(\Gamma) m_\Gamma^3 (1 + 2x) e^{-2x} \tag{A39}
\end{aligned}
$$

where x is the scaling variable defined in (A34).

Finally, using $\rho_\Gamma(\Gamma) = 2A\Gamma^{\mu-1}$ and the new variable x as integration variable instead of Γ, we obtain the magnetization per spin (A35) as

$$
m_{spin}(h) = (1/2) \int_0^{+\infty} d\Gamma \rho_\Gamma(\Gamma) m_\Gamma \left[1 + 2x \right] e^{-2x} \tag{A40}
$$

and the result

$$
m_{spin}(h) = h^{\frac{\mu}{\mu+2}} \left(\frac{4A}{\mu} \right)^{\frac{1}{\mu+2}} c_{simple}(\mu) \tag{A41}
$$

The exponents in h and A agree with the exact results of [5], whereas the prefactor reads

$$c_{simple}(\mu) \quad = \frac{\mu}{2(\mu+2)}\int_0^{+\infty} dx\, x^{\frac{\mu}{\mu+2}-1}(1+2x)e^{-2x} == \frac{1+\mu}{2+\mu}2^{-\frac{\mu}{\mu+2}}\Gamma\left(1+\frac{\mu}{\mu+2}\right) \tag{A42}$$

$$= \frac{1}{2} + \mu\frac{1-\gamma_{Euler}-\ln 2}{4} + \mu^2\left[\frac{(\gamma_{Euler}+\ln 2)^2}{16} - \frac{12-\pi^2}{96}\right] + O(\mu^3) \tag{A43}$$

instead of the exact prefactor obtained via transfer matrix computations [5] that reads in our notations

$$c_{exact}(\mu) = (\mu+2)^{-\frac{2}{\mu+2}}(\mu+1)\frac{\Gamma\left(\frac{\mu+1}{\mu+2}\right)}{\Gamma\left(\frac{1}{\mu+2}\right)} = \frac{1}{2} + \mu\frac{1-\gamma_{Euler}-\ln 2}{4} + \mu^2\frac{(\gamma_{Euler}+\ln 2)^2}{16} + O(\mu^3) \tag{A44}$$

so the discrepancy with the exact prefactor (A44) only appears at order μ^2.

---

[1] Y. Imry and S. K. Ma, Phys. Rev. Lett. **35**, 1399 (1975).
[2] D. S. Fisher, P. Le Doussal and C. Monthus, Phys. Rev. **E64**, 66107 (2001).
[3] C. Monthus and P. Le Doussal, cond-mat/0407289.
[4] H.H. Chen and S.K. Ma, J. Stat. Phys. **29**, 717 (1982).
[5] E. Gardner and B. Derrida, J. Stat. Phys. **39**, 367 (1985).
[6] P.W. Anderson, B.I. Halperin, C.M. Varma, Phil. Mag. **25** , 1 (1972).
[7] J. Houdayer, private communication.
[8] S.N. Majumdar and P.L. Krapivsky, Phys. Rev. **E65**, 036127 (2002); D.S. Dean and S.N. Majumdar, J. Phys. **A35**, L501 (2002).
[9] I. Morgenstern, K. Binder and R.M. Hornreich, Phys. Rev. **B23**, 287 (1981).
[10] K. Binder, Z. Phys. **B50**, 343 (1983); P. Shukla, cond-mat/0401253
[11] F. Barahona, R. Maynard, R. Rammal and J.P. Uhry, J. Phys. **A15**, 673 (1982).
[12] B. Derrida and G. Weisbuch, Europhys. Lett. **4**, 657 (1987).
[13] I.A. Campbell and L. de Arcangelis, Europhys. Lett. **13**, 587 (1990).
[14] T. Klotz and S. Kobe, J Phys **A27**, L95 (1994).
[15] G. Hed, A. K. Hartmann, D. Stauffer, and E. Domany Phys. Rev. Lett. **86**, 3148 (2001); E. Domany, G. Hed, M. Palassini, and A. P. Young Phys. Rev. **B64**, 224406 (2001); G. Hed, A. P. Young, and E. Domany Phys. Rev. Lett. **92**, 157201 (2004).
[16] E Domany, G. Hed, private communication.